ELSEVIER

Surface Science 426 (1999) 26–37

surface science

www.elsevier.nl/locate/susc

Systematic theoretical studies of the Schottky barrier control by passivating atomic intralayers

R. Saiz-Pardo, R. Pérez *, F.J. García-Vidal, R. Whittle, F. Flores

Departamento de Física Teórica de la Materia Condensada, Facultad de Ciencias, Universidad Autónoma de Madrid, E-28049 Madrid, Spain

Received 27 November 1998; accepted for publication 4 January 1999

Abstract

The effect of different atomic intralayers on the Schottky barrier height ϕ_{bn} of covalent and ionic semiconductors has been studied theoretically. The following cases have been analysed: H/Si(111), Sb/Si(111), S/Ge(100), H/GaAs(110), Sb/GaAs(110) and As/GaAs(110). Our results show that ϕ_{bn} is reduced by all the intralayers and that this reduction increases with the intralayer electronegativity and the semiconductor ionicity. These results are explained by the chemical interaction between the adsorbed metal orbitals and the new levels associated with the passivating layer. This interaction shifts the semiconductor charge neutrality level to higher energies and, consequently, reduces the Schottky barrier height.

Keywords: Adatoms; Gallium arsenide; Germanium; Green's function methods; Interface states; Metal–semiconductor interfaces; Schottky barrier; Silicon

1. Introduction

The electronic properties of metal–semiconductor interfaces have been extensively studied since the discovery of their rectifying behaviour [1–7]. Since the application of synchrotron radiation to the characterization of these interfaces, important advances have been reached in our understanding of the Schottky barrier formation [6,8,9]. In particular, the metal–semiconductor junction has been analysed by progressively depositing a metal overlayer on the semiconductor [8–11]. These studies have allowed researchers to discriminate among different competing models trying to explain the junction behaviour and, eventually, a relatively broad consensus in the community has been reached attributing different mechanisms either to the induced density of interface states (IDIS) [12–14] or to the defects [15–17] existing at the very same interface.

Ideal (defect free) metal–semiconductor interfaces are now accepted as being controlled in their electronic properties by the IDIS created at the junction when a metal overlayer is deposited on the semiconductor (this is called IDIS model [13] or, alternatively, the virtual gap states model [2]). The interface Fermi level position will depend primarily on the intrinsic charge neutrality level (CNL) derived from the semiconductor band structure, as discussed in Refs. [13,14].

Then, when experimental conditions can be controlled to reduce the interface defect density of states to below $10^{13}\,cm^{-2}$, the Schottky barrier height is determined by the IDIS. In highly

* Fax: +34 91-3974950.
E-mail address: ruben@uamca5.fmc.uam.es (R. Pérez)

0039-6028/99/$ – see front matter
PII: S0039-6028(99)00179-X

defective interfaces, however, the barrier height is controlled by the defect states if at least some of them are charged [15–17], as proposed in the unified defect model (UDM).

This conclusion is also based on the analysis of the chemical bonds associated with the atoms of the semiconductor last layer bonded to the deposited metal atoms. In other words, this line of thought suggests that the Schottky barrier height is controlled by the semiconductor surface dangling bonds and that, by modifying these dangling bonds (with defects or in some other way), one can control the barrier height.

The simplest approach to this procedure is to passivate the semiconductor surface before depositing the metal film [18]. We can expect that this passivation will alter the semiconductor surface properties and, consequently, the Schottky barrier height [19–22]; similar ideas have also been implemented for heterojunctions, see Ref. [23].

In this paper we explore this idea by analysing theoretically different passivated semiconductor surfaces, looking for some general results that might offer a guide to the control of the Schottky barriers. We analyse different covalent and ionic semiconductors. In particular we have studied: (a) the following covalent interfaces, H/Si(111), Sb/Si(111) $\sqrt{3}\times\sqrt{3}\,30^{\circ}$, S/Si(100) and S/Ge(100); these cases include two semiconductors, Si and Ge, and several adatoms, H, Sb and S, with increasing electronegativity; (b) the interfaces, H/GaAs(110), As/GaAs(110) and Sb/GaAs(110), having also adatoms with different electronegativities [25–27].

A full analysis of all these cases offers the possibility of finding trends that we shall discuss at the end of the paper. We should say that in this analysis we study the modification of the Schottky barrier height considering only the case of a K–semiconductor or a K-adlayer–semiconductor interface. Although other metals can yield different Schottky barriers, the prototypical case of K is sufficient to understand the main changes induced by the passivating layer. We should also say that possible effects associated with the metallization of the metal overlayer (a kind of metal–insulator transition, depending on the metal coverage) have been neglected in this analysis [4,5,7]. Although they are important for understanding the very low coverage limit, it has been shown elsewhere [28] that a metal monolayer is sufficient for pinning the Fermi level at the position it reaches for a large metal coverage. Moreover, even for lower coverages, where correlation effects may render the overlayer not to be metallic (as might occur for half a monolayer of Cs deposited on GaAs(110) [29]), the mean field solution provides a metallic interface and a Schottky barrier height that is in very good agreement with the value calculated for a full coverage.

Some experimental groups have already analysed the effect of different intralayers on the Schottky barrier height [19–22]. We mention, for their direct relation with the results presented here, the work of Zahn et al. [30] for the Ag/Sb/GaAs(110) interface and the work of Kampen et al. [31] for the Ag/H/Si(111) contact.

In Section 2 we discuss briefly the method we have used to calculate different interfaces, and in Section 3 we present our main calculations. Finally, in Section 4 we discuss our results and present our conclusions.

2. Method of calculation

The analysis of the structure and the electronic properties of the different interfaces is based on a first-principles LCAO Hamiltonian that has been solved self-consistently using the orbital occupancy approximation (LCAO-OO or LCAO3) [32–35].

In this approach the LCAO Hamiltonian is split into its one-electron and many-body contributions:

$$\hat{H}=\hat{H}^{\mathrm{o.e.}}+\hat{H}^{\mathrm{m.b.}}, \tag{1}$$

where

$$\hat{H}^{\mathrm{o.e.}}=\sum_{i\sigma}E_{i\sigma}\hat{n}_{i\sigma}+\sum_{i\neq j\sigma}T_{ij\sigma}(\hat{c}_{i\sigma}+\hat{c}_{j\sigma}+\hat{c}_{j\sigma}+\hat{c}_{i\sigma}), \tag{2}$$

and

$$\hat{H}^{\mathrm{m.b.}}=\sum_{i}U_{i}^{(0)}\hat{n}_{i\uparrow}\hat{n}_{i\downarrow}+\frac{1}{2}\sum_{i\neq j\sigma}(J_{ij}^{(0)}\hat{n}_{i\sigma}\hat{n}_{j\bar{\sigma}}+\tilde{J}_{ij}^{(0)}\hat{n}_{i\sigma}\hat{n}_{j\sigma}). \tag{3}$$

In these equations $E_{i\sigma}$ represents the different orbital levels and $T_{ij\sigma}$ the hopping integrals in the orthogonal basis ϕ_i obtained by a Löwdin transformation, $\phi_i = \Sigma_j (S^{-1/2})_{ij} \psi_j$, from the valence atomic wavefunctions ψ_j of the different atoms in the system. The effect of the core orbitals is included in both the diagonal levels and the hopping integrals using an effective pseudopotential, as explained in Ref. [35]. The expressions $U_i^{(0)}$, $J_{ij}^{(0)}$, and $\tilde{J}_{ij}^{(0)}$ define the intrasite and intersite Coulomb interactions associated with the atomic orbitals. In $\tilde{J}_{ij}^{(0)}$ the bare intersite Hartree term is corrected by the exchange interaction. Notice that $J_{ij}^{(0)}$ and $\tilde{J}_{ij}^{(0)}$ include all the long-range Coulomb interactions between electron charges that play a crucial role in the formation of the metal–semiconductor interface. This long-range electrostatic potential is responsible for the dipole, induced by the charge transfer between the metal and the semiconductor, that shifts the electron energy levels. As discussed in Ref. [13], it is the balance between the charge transfer and the induced interface dipole which brings the metal Fermi energy close to the semiconductor CNL. This stresses the importance of including in a self-consistent way the potential created by the induced charges, as done in our method (see below). Different parameters of the Hamiltonian in Eq. (1) are calculated as discussed in Ref. [33] for describing the interaction between layers located around the interface. Inside the semiconductor, the Hamiltonian in Eq. (2) is taken from the semi-empirical parameters of Refs. [36,37].

The many-body Hamiltonian is treated using an orbital-occupancy (OO) approximation, where the occupation numbers $n_{i\sigma}$ ($n_{i\sigma} = \langle \tilde{n}_{i\sigma} \rangle$, where $\langle\rangle$ is the expectation value in the ground state), associated with the different orbitals $\phi_{i\sigma}$, take the role that the electron density $\rho(\boldsymbol{r})$ plays in the Kohn–Sham formalism used in density functional theory (DFT). This means the introduction of an effective one-electron Hamiltonian

$$\hat{H} = \hat{H}^{\text{o.e.}} + \sum_{i\sigma} (V_{i\sigma}^{\text{H}} + V_{i\sigma}^{\text{XC}}) \hat{n}_{i\sigma} \tag{4}$$

where a local potential for each orbital is defined from the many-body terms of the Hamiltonian. This local potential has both Hartree, $V_{i\sigma}^{\text{H}} = U_i^{(0)} n_{i\bar{\sigma}} + \Sigma_{i \neq j\sigma'} J_{ij}^{(0)} n_{j\sigma'}$, and exchange-correlation $V_{i\sigma}^{\text{XC}} = \partial E^{\text{XC}} / \partial n_{i\sigma}$, contributions, where the exchange-correlation energy E^{XC} is shown to be a function of the occupation numbers $n_{i\sigma}$. A detailed discussion, of the procedure can be found in Ref. [34]. This effective Hamiltonian is solved self-consistently using Green's function techniques for the determination of the ground state and the calculation of the occupation numbers $n_{i\sigma}$. From this solution we can calculate the total energy of the system, as in standard DFT, by adding the one-electron and many-body energies:

$$E_{\text{tot}} = E_{\text{BS}} - E_{\text{DC}} + E_{\text{ion–ion}} + E^{\text{XC}} - \sum_{i\sigma} V_{i\sigma}^{\text{XC}} n_{i\sigma}. \tag{5}$$

The first term of Eq. (5), E_{BS}, is the band structure energy (the sum of the occupied eigenvalues of the effective hamiltonian); E_{DC} is the double-counting correction for the Hartree contributions, and $E_{\text{ion–ion}}$ is the repulsive interaction between the ions.

The use of Green's function techniques allows us to describe the interactions among the metal layer, the passivating intralayers and the last four semiconductor layers, as well as their interaction with a semi-infinite semiconductor material [38]. The system has surface (2D) periodicity and $\boldsymbol{k}$-point sampling techniques [39] are used for the determination of the occupation numbers, the local density of states (LDOS) for the different atoms and the band-structure energy.

A structural relaxation for the different systems considered has been performed looking for the minimum of the total energy. The chemisorption energy is defined as the difference between the total energy at that minimum and the sum of the total energy of the bare surface and the total energy of the isolated atoms for the different adsorbed species.

3. Results for covalent and ionic semiconductor surfaces

3.1. Covalent semiconductors

The following cases have been analysed: H/Si(111), Sb/Si(111), S/Si(100) and S/Ge(100).

3.1.1. H/Si(111)

Hydrogen is well-known to saturate the dangling bonds of the Si(111) surface forming then an ideal 1×1 geometry [40,41]. Our calculated chemisorption energy per H-atom is 2.7 eV, and the different LDOS for the H- and the last Si-layer are shown in Fig. 1 (top panel). Notice the excellent passivation this surface shows, with no density of states in the energy region between 0 and 1.1 eV above the semiconductor valence band top.

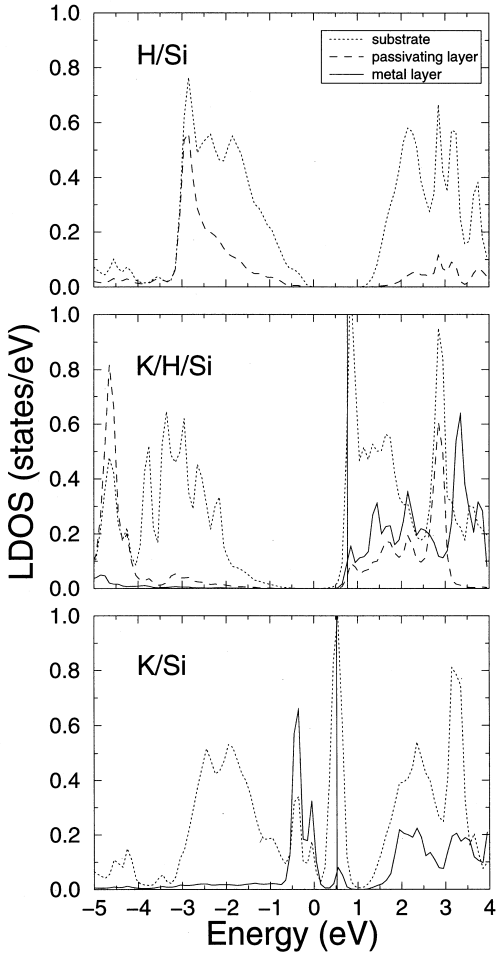

Fig. 1. LDOS (in units of states/eV) for the H/Si(111) (top panel), K/H/Si(111) (central panel) and K/Si(111) (bottom panel) interfaces. In each case, the LDOS per atom in the last substrate layer (dotted line), the passivating layer (dashed line) and the metal layer (solid line) are shown. The straight vertical line marks the position of the Fermi level. $E=0$ corresponds to the semiconductor valence band maximum (VBM).

Metallization of this surface can be reached by, for example, depositing K on it. We have calculated the K/H/Si(111) interface by assuming a $\sqrt{3}\times\sqrt{3}$ geometry for the K-monolayer, and have looked for the most favourable geometry by minimizing the total energy. We have found that the threefold adsorption site (usually known as H_3) yields the most energetically favourable position for K, with a chemisorption energy of 0.53 eV per K-atom and a K–H distance of 2.3 Å. Fig. 1 (central panel) shows the LDOS of that K-most favourable position for the K, H and the Si-last layer. The important point to notice is that the Fermi level is pinned, at around 0.78 eV, by the density of states induced by the metal in the upper part of the semiconductor energy gap. The K-density of states has also a small contribution overlapping with the semiconductor valence band with a total charge of 0.34 electrons per atom. This is associated with an important charge transfer of 0.66 electrons per atom going from the alkali metal atom to the semiconductor. It is also clear, from the comparison of the LDOS in Fig. 1, that the effect of the K-monolayer is to push to lower (more binding) energies the density of states associated with the H and Si atoms.

In order to understand how passivation has altered the Schottky barrier formation, we have also studied the K/Si(111) interface for an alkali metal monolayer having a $\sqrt{3}\times\sqrt{3}$ geometry. This geometry has been found when depositing Cs on an Si(111)-2×1 reconstruction [42]. Although K does not seem to form the $\sqrt{3}\times\sqrt{3}$ structure [43], it is known that the Schottky barrier heights for K do not change significantly with the adsorption geometry; therefore, we have considered that structure for the sake of comparison with the passivated surface, in order to understand its effect on the Schottky barrier formation. The bottom panel of Fig. 1 shows the LDOS for the K–Si(111) interface with the Fermi level pinned at 0.52 eV by the density of states resulting from the interaction between the ideal Si(111)-surface states and the K-level. In this calculation, the K chemisorption energy is 2.4 eV, and the K charge transfer to the semiconductor is 0.35 electrons. The comparison with the other LDOS in Fig. 1 shows that: (i) the

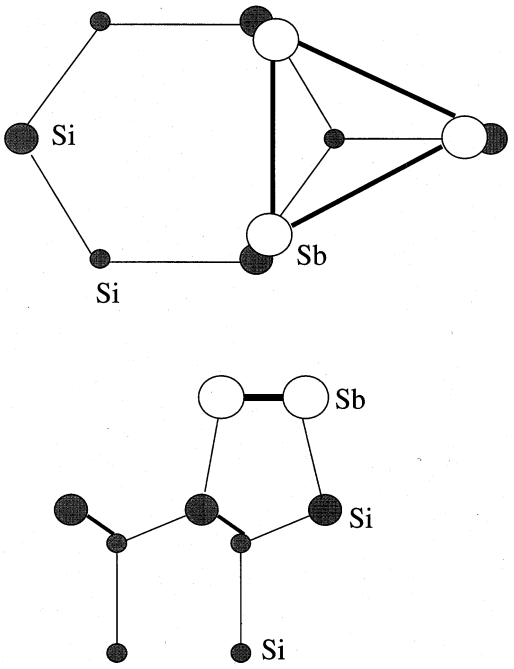

Fig. 2. Surface geometry for the Sb/Si(111) reconstructed surface.

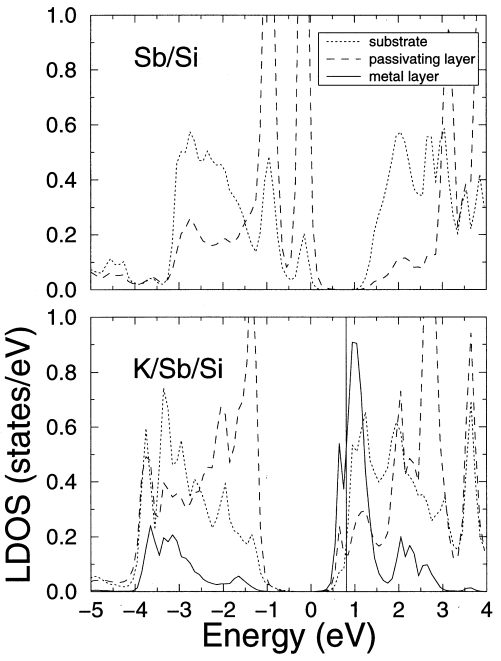

Fig. 3. LDOS for the Sb/Si(111) (top panel) and K/Sb/Si(111) (bottom panel) interfaces (details as in Fig. 1).

Fermi level for the passivated surface has moved up from 0.52 eV to 0.78 eV, and (ii) that this effect is mainly due to the interaction of the H-density of states with the K-level, which makes the K-band controlling the position of the Fermi level move towards higher (less binding) energy with respect to its position in the clean K/Si(111) interface.

3.1.2. Sb/Si(111)

Sb also passivates Si surfaces. LEED and STM studies have identified different surface geometries, with either a $\sqrt{3}\times\sqrt{3}$R30° or a 2×1 reconstruction [44,45]. In our calculations, we have found both reconstructions to have similar chemisorption energies, although the one shown in Fig. 2 yields a global marginal minimum around 2.9 eV per Sb atom and, therefore, it defines the passivated surface we take for analysing the Sb/Si(111) interface.

Fig. 3 (top panel) shows the LDOS we have calculated for the Sb and the last Si-layer, for the geometry shown in Fig. 2. Notice that, in our calculations, the passivation of the Si surface is not perfect with some density of states filling the lower part of the semiconductor energy gap. These states are associated with the Sb-lone pairs that are directed towards the vacuum side. Notice, in this regard, that each Sb atom forms one bond with an Si atom and two bonds with two Sb atoms. Three valence electrons, out of five, contribute to these bonds while the other two valence electrons fill the lone pair whose density of states appears at the semiconductor valence band top.

The K–Sb–Si(111) $\sqrt{3}\times\sqrt{3}$ interface LDOS is shown in Fig. 3 (central panel). The K-atoms are assumed also to form a $\sqrt{3}\times\sqrt{3}$ reconstruction. Our calculations favour the A-site shown in Fig. 2 for the K-position, although we should point out that, in this case, our calculated binding energy per K-atom is only around 0.1 eV. This might be taken as an indication of the difficulty of growing K on the passivated Sb/Si(111) $\sqrt{3}\times\sqrt{3}$ interface. In spite of this result, our calculation of the K/Sb/Si(111) interface can be used for analysing the effect of the Sb-passivation on the Si(111) Schottky barrier height. The results of Fig. 3 (bottom panel) show that the K deposition creates

a new density of states near the semiconductor conduction band bottom, pinning the Fermi level at 0.81 eV above the semiconductor valence band top. At the same time, a comparison between the two panels in Fig. 3 shows that another effect of the K-deposition is to push downwards in energy the LDOS associated with the Sb and Si atoms. Moreover, this interaction also tends to pull up in energy the LDOS that we calculated previously in the K/Si(111) interface (see bottom panel of Fig. 1). The result of all these interactions is that the Fermi energy, which for the K/Si(111) interface is located at 0.52 eV, is shifted up to 0.81 eV for the Sb-passivated Si surface.

3.1.3. S/Ge(100)

Next, we have analysed the effect of sulfur on the Ge(100) surface. This surface is known to present a 2×1 reconstruction with the surface atoms forming dimers. The deposition of S seems to remove this dimerization, with the Ge atoms returning to nearly their bulk positions [46,47]. In our calculations of this system the energy gained per S atom is 1.9 eV with respect to the symmetrically dimerized Ge surface. Fig. 5 (top panel) shows our calculated LDOS for the S and the Ge-last layer. These results clearly show that the nominally passivated S/Ge(100) surface does not remove completely the density of states from the semiconductor energy gap. Our calculations are in reasonable agreement with plane wave DFT-LDA calculations [47], although a GW-approximation leads to the opening of a band gap of about 0.15 eV [48]. Our calculations for this S/Ge(100) surface yield a Fermi level located about 0.62 eV above the bulk valence band maximum (VBM). We should mention that, although the S/Ge(100) surface seems to be metallic, the density of states in the band gap is low, with the main surface-related peaks of the Ge(100)-(2×1) reconstruction almost completely sweeping out of the gap. While not entirely passivated, this interface has far fewer gap states than the calculated clean Ge surface, and should be significantly less reactive.

The Schottky barrier formation of this interface is also studied by depositing K. We consider a (1×1) geometry with the K atoms located in the adsorption sites shown in Fig. 4, where the geometries of the S–Ge(100) and the K–S–Ge(100) interfaces are shown. Our calculations clearly favour the bridge position, with an adsorption energy of 1.12 eV (to be compared with 0.61 eV, 0.4 eV and 0.26 eV for the top, hollow and antibridge sites respectively). Fig. 5 (central panel) shows our calculated LDOS for the K, S and the Ge top layer; in this calculation the Fermi level is located at 0.66 eV above the semiconductor VBM. Comparing with the top panel of Fig. 5, where the LDOS for the S–Ge(100) is shown, we find similar results to the ones reported above; in particular, K is inducing a density of states where the Fermi level is pinned and, secondly, the interaction between the K-level and S or Ge pushes down to lower energies the electronic structure appearing near the semiconductor energy gap and associated with either S or Ge. This same interaction prevents the Fermi level going down in energy to the position found for the K–Ge(100) interface.

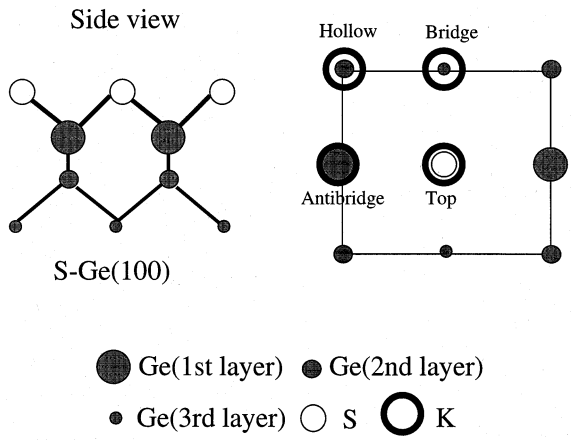

Fig. 4. Different adsorption sites for K (labelled A–B) on the S/Ge(100) passivated interface.

This particular case [K on Ge(100)] has been analysed in order to find a reference Fermi level with which to compare previous results. We performed calculations with K coverages of 0.5 monolayers, with the K atoms located in a number of possible sites on the dimerized 2×1 surface. This low K-coverage can be used, as it has been previously shown that the Fermi level is essentially determined at the onset of metallization, which in our case occurs at 0.5 monolayers. We find that

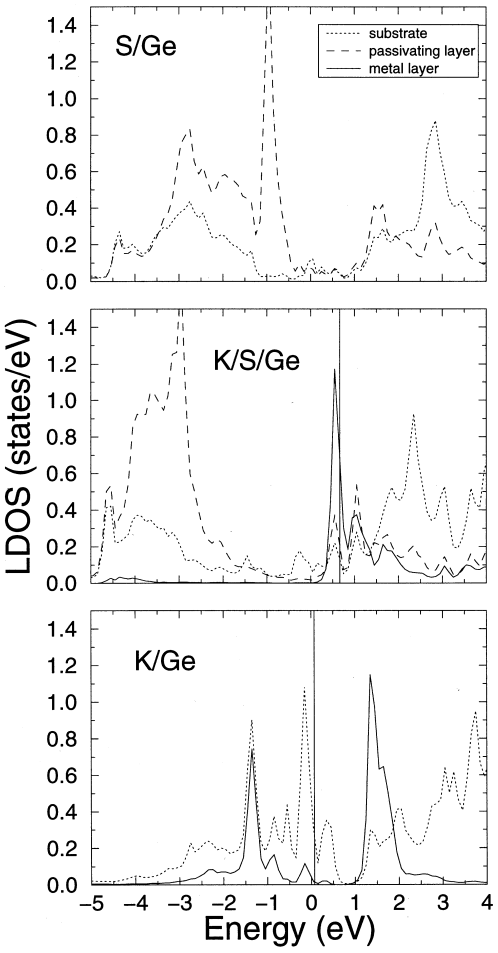

Fig. 5. LDOS for the S/Ge(100) (top panel), K/S/Ge(100) (central panel) and K/Ge(100) (bottom panel) interfaces (details as in Fig. 1).

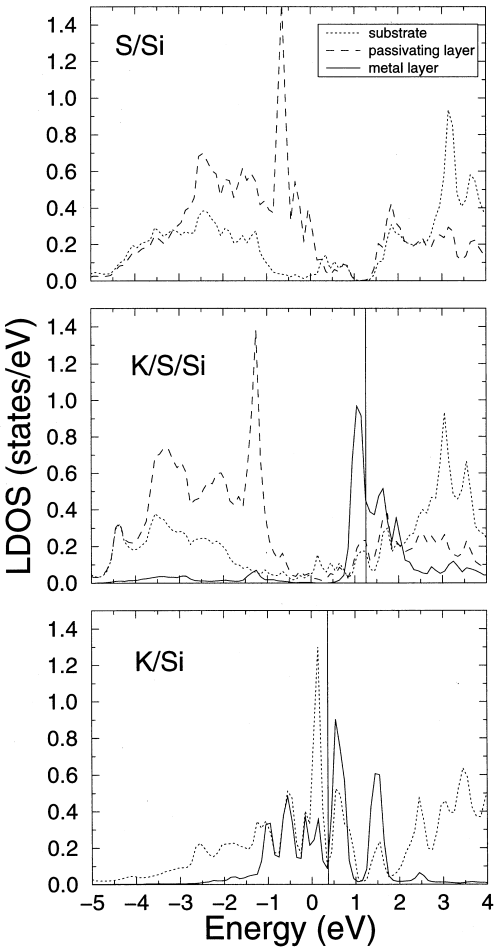

Fig. 6. LDOS for the S/Si(100) (top panel), K/S/Si(100) (central panel) and K/Si(100) (bottom panel) interfaces (details as in Fig. 1).

the energetically preferred site is the so called T_3 site, in agreement with other calculations [49]. We have checked that the position of the Fermi level does not vary greatly for the different bonding sites. Fig. 5 (bottom panel) shows the LDOS for the K/Ge(100) 2×1 interface; here the Fermi level is located at 0.17 eV above the valence band top. It is also interesting to compare the different panels in Fig. 5; from this comparison we conclude that the S–K interaction pushes up to higher energies the K-induced density of states in the semiconductor energy gap and yields a Fermi energy level that is located for the K/S/Ge interface 0.49 eV above the one found for the K/Ge case.

3.1.4. S/Si(100)

Finally, we have also studied the S/Si(100) interface, which shows large similarities to the S/Ge(100) case. Without going into many details, we show in Fig. 6 our main results for the LDOS of the different cases: S/Si(100), K/S/Si(100) and K/Si(100). From those results, we deduce that the Fermi level for the K/S/Si(100) and the K/Si(100) interfaces are located at 1.26 eV and 0.37 eV respectively above the VBM. It must be noted that

the Fermi level pinning at a position above the conduction band minimum (CBM) is due to the use of a restricted self-consistency in the semiconductor overlayer. A thicker semiconductor overlayer will provide an ohmic contact with the Fermi level pinned right at the semiconductor CBM, which in our calculation is located at 1.12 eV above the VBM. Taking this into account, our calculation shows that the effect of S-passivation is to modify the Fermi level position by 0.75 eV, moving it, as in previous cases, in the higher (lower binding) energy direction. We should only comment at this point that the LDOS calculated for the different interfaces shows striking similarities with the Ge case discussed above. In particular, we also find for the K/S/Si(100) interface that the Fermi level shift is basically due to the interaction between the K-level and the LDOS associated with the passivating layer. However, in the K/S/Ge interface the Fermi level is pinned below the CBM, not forming an ohmic contact as in the K/S/Si case.

3.2. Ionic semiconductors

The following cases have been analysed: H/GaAs(110), Sb/GaAs(110) and As/GaAs(110).

3.2.1. H/GaAs(110)

This interface has been analysed by different groups [50,51]. The evidence tends to support the interpretation that H chemisorbs on both As and Ga with similar bond strengths; then we can expect the H atoms to be equally deposited on the two semiconductor dangling bonds. We have analysed this interface by assuming the H-monolayer to saturate both the Ga and As dangling bonds. This saturated monolayer has a binding energy to the substrate of 2.4 eV per H-atom [34]. Fig. 7 shows its LDOS in the H and the GaAs top layer; this figure shows the good saturation H achieves for the semiconductor with no density of states in the GaAs energy gap.

In a further step, we have studied the Schottky barrier formation by considering the K/H/GaAs(110) interface. Our calculation yields that the K-atoms of the first monolayer are located preferentially on a threefold symmetry position, coordinated to three H atoms (see Fig. 8). For this

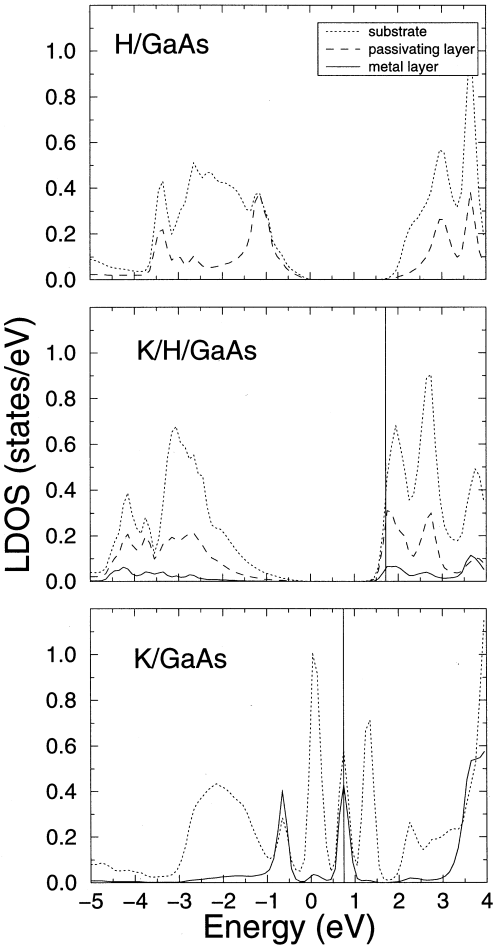

Fig. 7. LDOS for the H/GaAs(110) (top panel), K/H/GaAs(110) (central panel) and K/GaAs(110) (bottom panel) interfaces (details as in Fig. 1).

geometry we find the LDOS shown in Fig. 7 (central panel). This figure shows how the K-monolayer induces a density of states located in the upper part of the semiconductor energy gap. Our results yield, however, a Fermi level that is just above the semiconductor CBM. This indicates, as explained above for the S/Si(110) case, that the H-passivated GaAs surface yields an ohmic contact to a metal.

For the sake of comparison, we have also studied the K/GaAs(110) interface [52]. Fig. 7 (bottom panel) shows our calculated LDOS in H and the Ga and As atoms of the top-most semicon-

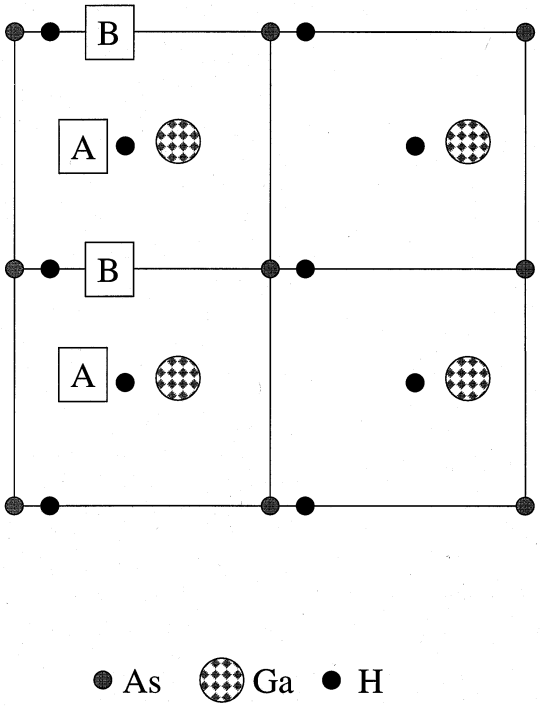

Fig. 8. Different adsorption sites (labelled A–D) for K on the H/GaAs(110) passivated interface.

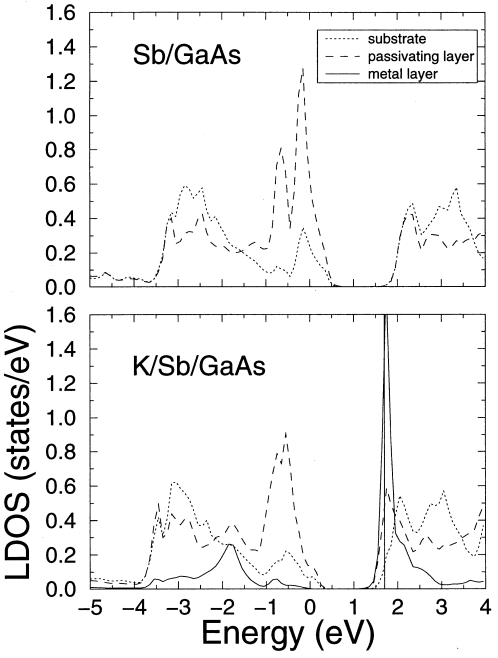

Fig. 9. LDOS for the Sb/GaAs(110) (top panel) and K/Sb/GaAs(110) (bottom panel) interfaces (details as in Fig. 1).

ductor layer. The K-atoms of the alkali metal monolayer are bonded to the Ga-atoms and form an ideal Schottky barrier with the K-induced states pinning the Fermi level at 0.75 eV above the semiconductor valence band top. The comparison between the different panels of Fig. 7 shows the effect of the H intralayer: the interaction between the H density of states for the saturated interface and K pushes up the K-induced density of states, shifting the Fermi level from 0.75 eV [K–GaAs(110) case] to around 1.45 eV [the K–H–GaAs(110) case].

3.2.2. Sb/GaAs(110)

From different experimental evidence [53,54] and theoretical studies [55], it is well known that Sb passivates the GaAs(110) surface. The first layer of Sb is located in the natural continuation of the ideal GaAs crystal, with the Sb atoms forming linear chains along the surface. The Sb deposition tends to eliminate the GaAs relaxation and, in the following calculations, we shall assume the GaAs surface to be the ideal unrelaxed one.

Fig. 9 shows our calculated LDOS for this Sb/GaAs(110) surface. Our results compare well with other calculations [55,56]. In particular, the first peak in the Sb-LDOS below the semiconductor energy gap is associated with the Sb lone pairs formed at the interface after the Sb bonding to one semiconductor atom (either As or Ga) and two other Sb atoms.

The results of Fig. 9 (top panel) show that this Sb–GaAs(110) interface is rather well saturated, although a small density of states (Sb-like surface bands) appears just above the semiconductor valence band top.

The metallization of this interface is simulated by a K-monolayer. Different geometries for an Sb monolayer have been studied (Fig. 10 shows the cases considered in this work). The chemisorption energy of the most favourable case is only 0.3 eV, indicating that the growth of K on the Sb/GaAs interface should be very difficult. However, we have analysed theoretically this ideal case since it

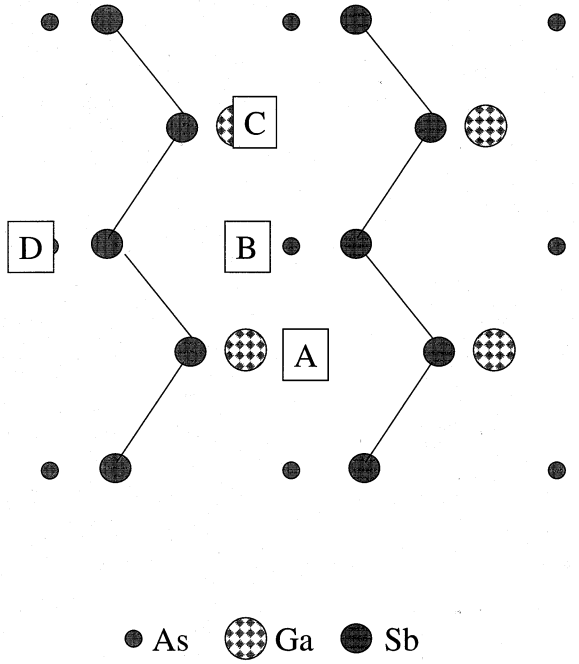

Fig. 10. Different adsorption sites (labelled A–D) for K on the Sb/GaAs(110) passivated interface.

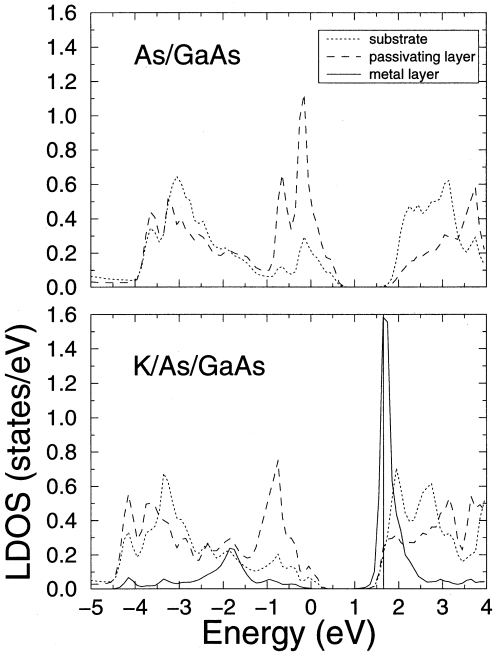

Fig. 11. LDOS for the As/GaAs(110) (top panel) and K/As/GaAs(110) (bottom panel) interfaces (details as in Fig. 1).

can give valuable information about its Schottky barrier formation. Fig. 9 (bottom panel) shows our calculated LDOS for the K/Sb/GaAs(110) most favourable geometry (this is the A position of Fig. 10). In this figure, we find the Fermi level at 1.50 eV above the valence band top, the metal forming an ohmic contact to the semiconductor. As in previous cases, this is the result of the interaction of K with the density of states associated with Sb. In this particular case, the Sb lone pairs are the orbitals more strongly interacting with the K conduction band and shifting the K-induced density of states and the Fermi level to higher energies, as shown in the bottom panel of Fig. 9.

3.2.3. *As/GaAs(110)*

We have also studied this interface assuming the same geometry as the Sb/GaAs(110) case, although the experimental evidence [57] shows a disordered surface structure suggesting that As does not form the ordered structure we have just analysed for Sb. We believe, however, that the following theoretical analysis will help us to understand the basic mechanism controlling the Schottky barrier formation. Fig. 11 shows our main results for the LDOS associated with the As/GaAs(110) and K/As/GaAs(110) interfaces. In general, we can conclude that both interfaces, the As/GaAs and the Sb/GaAs, show practically the same behaviour, this result being probably due to having assumed the same geometries for both cases.

Let us only mention that the main output of this calculation of the Schottky barrier height, which for the ideal K/GaAs junction is 0.75 eV (see bottom panel of Fig. 7), has increased to around 1.45 eV for this saturated As/GaAs interface.

4. Discussion and conclusions

The aim of this paper has been to study theoretically the effect of different atomic intralayers on the Schottky barrier height of covalent or ionic

semiconductors. We have analysed the following cases: H/Si(111), Sb/Si(111) $\sqrt{3}\times\sqrt{3}$ 30°, S/Si (100), S/Ge(100), H/GaAs(110), Sb/GaAs(110) and As/GaAs(110). Our results for these interfaces have shown that their Fermi level associated to a K-monolayer (referred to the semiconductor valence band top) has changed significantly from the ideal case (without the passivating intralayer) as shown in Table 1.

In all these cases we observe that the effect of the passivating intralayer has been to shift the Fermi level to higher energies and reducing the Schottky barrier height ϕ_{bn}. The results for GaAs are only indicative, because for all the intralayers analysed the metal–semiconductor contact is found to be ohmic, with zero barrier height. The main conclusion we can draw from Table 1 is that the barrier height is reduced by all the intralayers, and that this reduction seems to be a function of the intralayer electronegativity. Thus, for Si, an H-intralayer reduces ϕ_{bn} by 0.26 eV, whereas Sb and S introduce shifts of 0.29 eV and 0.75 eV respectively; in this particular case S (the most electronegative atom) introduces the largest modification of ϕ_{bn} and produces an ohmic contact. It is also interesting to realize that, for Ge, the effect of S in ϕ_{bn} is only of 0.49 eV, and a marginally rectifying contact is formed (the Ge gap is 0.70 eV in our calculation). These differences suggest that the same passivating intralayer introduces smaller changes in ϕ_{bn} as we move along a column in the periodic table.

For GaAs it is difficult to draw any clear conclusion from the point of view of the intralayer electronegativity, because in all the cases analysed in this paper we have found an ohmic metal–semiconductor contact. These results show, however, that the same intralayers introduce larger modifications of the Schottky barrier heights for ionic semiconductors than for covalent crystals.

Table 1
Changes in the Fermi level position (referred to the VBM) due to the passivating intralayer for the different interfaces

	δE_F (eV)
K/H/Si(111)	0.52→0.78
K/Sb/Si(111)	0.52→0.81
K/S/Si(100)	0.37→1.12
K/S/Ge(100)	0.17→0.66
K/H/GaAs	0.75→1.45
K/Sb/GaAs	0.75→1.45
K/As/GaAs	0.75→1.45

On the other hand, our previous discussion about the LDOS appearing at different interfaces has shown that the basic mechanism introducing the barrier height shift is the interaction between the adsorbed metal density of states and the new levels associated with the passivating layer. In all the cases analysed, this interaction moves the metal band to higher (less binding) energies and shifts the interface Fermi level as discussed above. This can be described in a different way by stating that the CNL of the semiconductor, defining the Fermi level pinning at the interface, is shifted up to higher energies by the intralayers. This new CNL has been called an extrinsic one, and has been discussed in detail in Refs. [28,58,59].

Finally, it is worth commenting on the experimental evidence that has been presented by several groups. Although in some cases, as for Ag on Sb/GaAs(110), it has been proved [30] that the metal deposition disrupts the passivated surface, in others, like H/Si(111), it has been found that the passivated surface is very stable upon the deposition of a metal layer. Kampen et al. [32] have found that in an H/Si(111) passivated surface the interface Fermi level is shifted by 0.25 eV in the direction of higher (lower binding) energies, which is in good agreement with the results presented in this paper. Zahn and coworkers [60,61], as well as Mönch's group [62], have recently presented some experimental evidence for GaAs(100) surfaces passivated by either S or Se. Although these cases are out of the scope of our work, it is worth mentioning that these authors have also observed for these interfaces a movement of the interface Fermi level in the direction of higher energies by 0.10–0.30 eV, in qualitative agreement with the results presented in this paper.

In conclusion, we have shown theoretically that the main effect of a passivating monolayer on the Schottky barrier formation is to reduce its height value ϕ_{bn}; this effect seems to depend on the intralayer electronegativity and the semiconductor

ionicity. In particular, the Schottky barrier height appears to be reduced when we increase either the intralayer electronegativity or the semiconductor ionicity.

Acknowledgements

We acknowledge financial support from the Spanish CICYT under contract number PB97-0028.

References

[1] F. Brown, Papp. Ann. 153 (1874) 556.
[2] W. Mönch, Electronic Structure of Metal–Semiconductor Contacts, Kluwer, Dordrecht, 1990.
[3] E.H. Rhoderich, R.H. Williams, Metal–Semiconductor Contacts, Oxford Science Publications, Oxford, 1988.
[4] F. Flores, C. Tejedor, J. Phys. C: Solid State Phys. 20 (1987) 145.
[5] F. Flores, Surf. Rev. Lett. 2 (1995) 513.
[6] L.J. Brillson, in: T.S. Moss (Ed.), Handbook of Semiconductors, Elsevier, 1992.
[7] F. Bechstedt, M. Scheffler, Surf. Sci. Rep. 18 (1993) 145.
[8] K. Stiles, A. Kahn, Phys. Rev. Lett. 60 (1988) 440.
[9] W.E. Spicer, Appl. Surf. Sci. 41–42 (1995) 513.
[10] M. Prietsch et al., Phys. Rev. Lett. 60 (1988) 436.
[11] M. Prietsch et al., Z. Phys. B 74 (1989) 21.
[12] V. Heine, Phys. Rev. 138 (1965) 1689.
[13] C. Tejedor, F. Flores, E. Louis, J. Phys. C: Solid State Phys. 10 (1977) 2163.
[14] J. Tersoff, Phys. Rev. Lett. 52 (1984) 465.
[15] W.E. Spicer et al., J. Vac. Sci. Technol. 17 (1979) 1019.
[16] R.H. Williams, J. Vac. Sci. Technol. 18 (1981) 929.
[17] W. Mönch, Surf. Sci. 132 (1983) 92.
[18] F. Flores, R. Miranda, Adv. Mater. 6 (1994) 540.
[19] J.R. Waldrop, Appl. Phys. Lett. 47 (1985) 1301.
[20] W. Mönch, Europhys. Lett. 27 (1994) 479.
[21] R. Berrigan et al., Jpn. J. Appl. Phys. 31 (1992) 3223.
[22] S. Tahatani, T. Kihawa, M. Nakazawa, Jpn. J. Appl. Phys. 30 (1991) 3763.
[23] P. Perfetti et al., Phys. Rev. Lett. 57 (1986) 2065.
[25] R. Saiz-Pardo et al., Surf. Sci. 307–309 (1984) 309.
[26] R. Saiz-Pardo et al., Appl. Surf. Sci. 92 (1996) 362.
[27] R. Saiz-Pardo et al., Surf. Sci. 123–124 (1998) 560.
[28] F. Flores, J. Ortega, Appl. Surf. Sci. 56–58 (1992) 301.
[29] L.J. Whitman, J.A. Stroscio, R.A. Dragoset, R.J. Cellota, Phys. Rev. Lett. 66 (1991) 1338.
[30] D.R.T. Zahn et al., Appl. Surf. Sci. 56 (1992) 228.
[31] T.U. Kampen et al., Appl. Phys. A 60 (1995) 391.
[32] E.C. Goldberg, A. Martín-Rodero, R. Monreal, F. Flores, Phys. Rev. B 39 (1988) 5684.
[33] F.J. García-Vidal, A.. Martín-Rodero, F. Flores, J. Ortega, R. Pérez, Phys. Rev. B 44 (1991) 11412.
[34] F.J. García-Vidal, J. Merino, R. Pérez, R. Rincón, J. Ortega, F. Flores, Phys. Rev. B 50 (1994) 10537.
[35] P. Pou, R. Pérez, J. Ortega, F. Flores, in: P.E.A. Turchi, A. Gonis, L. Colombo (Eds.), MRS 491 (1998) 45.
[36] D.A. Papaconstantopoulos, Handbook of the Band Structure of Elemental Solids, Plenum, New York, 1986.
[37] P. Vogel et al., J. Phys. Chem. Solids 44 (1983) 365.
[38] F. Guinea, C. Tejedor, F. Flores, E. Louis, Phys. Rev. B 28 (1983) 4397.
[39] S.L. Cunningham, Phys. Rev. B 10 (1974) 4988.
[40] K. Hricovini et al., Phys. Rev. Lett. 40 (1993) 1992.
[41] C.J. Karlsson et al., Phys. Rev. Lett. 72 (1994) 4145.
[42] K.O. Magnusson, B. Reihl, Phys. Rev. B 39 (1989) 10456.
[43] B. Reihl, K.O. Magnusson, Phys. Rev. B 42 (1990) 11839.
[44] C.Y. Park, Jpn. J. Appl. Phys. 27 (1988) 147.
[45] H.B. Elswijk, D. Dijkkamp, E.J. van Loeren, Phys. Rev. B 44 (1991) 3802.
[46] T. Weser et al., Surf. Sci. 201 (1988) 245.
[47] P. Kruger, J. Pollman, Phys. Rev. Lett. 64 (1990) 1808.
[48] M. Rohlfing, P. Kruger, J. Pollman, Phys. Rev. B 54 (1996) 13759.
[49] H.L. Megerheim, R. Sawitzky, W. Moritz, Phys. Rev. B 52 (1995) 16830.
[50] T.U. Kampen, Surf. Sci. 242 (1991) 314.
[51] H. Luth, R. Math, Phys. Rev. Lett. 46 (1981) 1652.
[52] J. Ortega, F. Flores, Phys. Rev. Lett. 63 (1989) 2500.
[53] C.B. Duke, A. Patou, W.K. Ford, Phys. Rev. B 26 (1982) 803.
[54] R.M. Feenstra, P. Martensson, Phys. Rev. Lett. 61 (1988) 447.
[55] C. Mailhiot, C.B. Duke, D.J. Chadi, Phys. Rev. B 31 (1985) 2213.
[56] W.G. Schmidt, F. Bechstedt, G.P. Srivatava, Surf. Sci. Rep. 25 (1996) 141.
[57] B. Kubler, W. Ranke, K. Jacobi, Surf. Sci. 92 (1980) 519.
[58] F. Flores, A. Muñoz, J.C. Durán, Appl. Surf. Sci. 41–42 (1989) 144.
[59] F. Gozzo et al., Solid State Commun. 81 (1992) 553.
[60] St. Hohenecker, T.U. Kampen, D.R.T. Zahn, J. Vac. Sci. Technol. in press.
[61] St. Hohenecker, D. Drews, M. Lubbe, D.R.T. Zahn, Appl. Surf. Sci. in press.
[62] W. Mönch et al., in: J. Lockwood (Ed.), Proc. 22nd Int. Conf. on the Physics of Semiconductors, World Scientific, Singapore, 1995.